therefore sheds light on the assumption that the positron's energy can be calculated as though it were always in a single state: that assumption *overestimates* the coefficient of the E^2-versus-$1/T$ curve by a factor 2.70, thereby *underestimating* the rate at which energy is lost.

For purposes of comparison, it is instructive to compute the value A would have if $F(P,T)$ were at all times a MB distribution corresponding to some temperature θ' higher than the sample temperature θ. In this case

$$F(P,T)=(4/\sqrt{\pi})(\theta/\theta')^{3/2}P^2\exp(-P^2\theta/\theta')$$

$$\int_0^\infty P^6F(P,T)=(\theta'/\theta)^3 3\times5\times(\tfrac{7}{2})^3 \qquad \text{(B11)}$$

$$\int_0^\infty P^2F(P,T)=(\theta'/\theta)^{\frac{3}{2}},$$

yielding

$$A=5\times(\tfrac{7}{2})=3.889. \qquad \text{(B12)}$$

If it were true, therefore, that the positron distribution was a M-B distribution for an effective temperature varying with time, the factor of disagreement between the present calculation and the calculation of Carbotte and Arora would *increase*.

The basis of the surprisingly large disagreement as to the value of the factor A in different distributions is the fact that A depends on the sixth moment of the distribution. It should be emphasized, however, that effective temperatures are estimated by setting $E(T_A)=\frac{3}{2}k\theta$. The estimated temperature therefore depends on the square root of the coefficient A. The factor of disagreement in the effective temperature is therefore $\sqrt{(2.70)}=1.64$. This factor is roughly compensated for by the effective-mass factor, so that the present predictions are close to those of Carbotte and Arora.

PHYSICAL REVIEW VOLUME 164, NUMBER 3 15 DECEMBER 1967

Modifications to the Orthogonalized-Plane-Wave Method for Use in Transition Metals: Electronic Band Structure of Niobium*

R. A. DEEGAN† AND W. D. TWOSE‡
Department of Physics, McMaster University, Hamilton, Ontario, Canada
(Received 10 July 1967)

Modifications to the orthogonalized-plane-wave (OPW) method are employed to facilitate its application to transition metals. The procedure is to augment the basis set of OPW's by including functions which vanish in the interstitial regions of the crystal but represent well the outer core functions and the d-band states near the nuclei. The bands are found to converge at a rate approximately the same as for the unmodified OPW method in semiconductors. The method is applied to calculate the conduction electron bands of niobium, along principal symmetry directions, to a convergence of about 0.01 Ry. The resulting band structure is very similar to previous augmented-plane-wave calculations for other bcc transition metals.

1. INTRODUCTION

THIS paper presents a method for calculating the electronic band structures of transition metals, based on modifications to the orthogonalized-plane-wave method. The modified method is applied to the transition metal niobium, for which convergence of the bands to about 0.01 Ry is obtained.

Difficulties in applying the OPW method to transition metals arise from: (1) the slow convergence for d-like conduction states[1]; and (2) the fact that the outermost s and p core states[2] are not completely localized but form bands of nonzero width. Problem (1) occurs because the wave function of a d state is not well represented by the $l=2$ component of a plane wave, even if the latter has been orthogonalized to a core level of d character. Problem (2) prevents orthogonalization of the plane waves to the outer core levels in the usual manner.

Following a suggestion by Herring,[3] which was later used by Callaway,[4] the d-band convergence is improved by adding to the basis set of OPW's a function which represents well the behavior of the d conduction band states in the inner region of the core but which is chosen to vanish in the interstitial regions. Similar cutoff (CO) functions are added to the basis set to represent the behavior of the outer core s- and p-wave functions, while the plane waves are orthogonalized to only those

* Based on a thesis submitted by R. A. D. in partial fulfilment of the requirements for the Ph.D. degree. This work was financially supported in part by the National Research Council of Canada.
† Present address: Cavendish Laboratory, University of Cambridge, Free School Lane, Cambridge, England.
‡ Dr. Twose died on April 5, 1967.
[1] Herman found that, for the $\Gamma_{25'}$ (d-like) state in diamond, a 16th order reduced secular equation (296 OPW's) was required to give the energy to within a few percent of convergence: F. Herman, Phys. Rev. **93**, 1214 (1954).
[2] Throughout this paper the term *core states* is used to designate the corelike eigenfunctions of the one-electron conduction band crystal Hamiltonian.
[3] C. Herring, Phys. Rev. **57**, 1169 (1940).
[4] J. Callaway, Phys. Rev. **97**, 933 (1955); **99**, 500 (1955).

core levels that are completely localized (which will be referred to here as inner core levels). The CO functions are explicitly orthogonalized to the inner core levels. With this basis set, the lowest roots of the secular equation in the variational calculation correspond to the outer core bands, while higher roots give the conduction bands. Because the outer core bands are quite narrow, the s and p CO functions can readily be chosen to be close approximations to the true wave functions of these states and therefore the convergence to these core bands (which, of course, is necessary before the higher roots can converge to the conduction bands) is quite fast.

Section 2 contains a more detailed description of the difficulties which arise in applying the OPW method to transition metals and the present modifications to treat them. The application of this modified method to niobium, including discussions on the convergence of the method and the resulting band structure, is then presented.

2. THEORY

A qualitative discussion of the two main difficulties and the manner in which each of them will be treated is given first. This is followed by an explicit statement of the modifications and the required matrix elements.

A. d Bands and OPW's

It was stated above that the d bands converge slowly because the wave function of a d state is not well represented by the $l=2$ component of an OPW. In order to display this for a typical d state, an example is presented in detail in Appendix A. The results are now summarized and discussed.

The example concerns niobium, which has an atomic configuration, outside closed shells, of $(4d)^4(5s)$. The d-like conduction bands in the metal, which is bcc, arise from the $4d$ states, while the core contains $3d$ states. As a typical point consider $\mathbf{k}=(2\pi/a)(\frac{1}{2},0,0)$ on the Δ_2 band. This state has no $l=0$ or 1 components and is dominantly $l=2$. The lowest symmetrized combination of plane waves with the correct symmetry for this state has a wave-vector magnitude $K=(2\pi/a)(\frac{5}{4})^{1/2}$. Consider one unit cell at the origin of direct space, and expand the OPW's in spherical harmonics about the center of this cell. The $l=0$ and 1 components of this symmetrized combination vanish. The radial part of the $l=2$ component is $j_2(Kr)$, the spherical Bessel function. The function $rj_2(Kr)$ is plotted in Fig. 1(a) for r ranging from zero to half the nearest-neighbor distance in niobium.

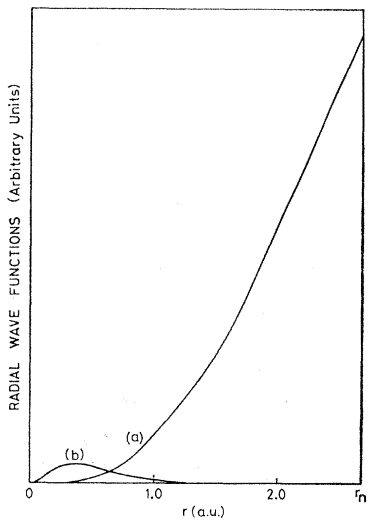

FIG. 1. For a typical d state in niobium [$\mathbf{k}=(2\pi/a)(\frac{1}{2},0,0)$ on the Δ_2 band]: Curve (a) is the radial wave function of the lowest symmetrized combination of plane waves. Curve (b) is the radial wave function of the $3d$ core state, after multiplication by an orthogonality constant so that it is of the correct amplitude to be subtracted from (a) to give the radial wave function of the lowest symmetrized combination of OPW's. [r is in atomic units (Bohr radii), and r_n is half the nearest-neighbor distance.]

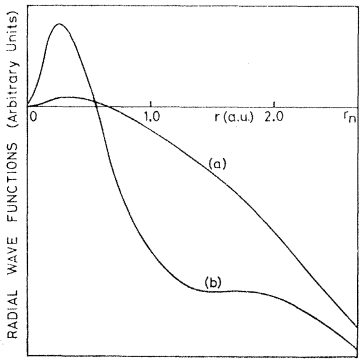

FIG. 2. For the d state considered in Fig. 1: Curve (a) is the radial wave function of the lowest symmetrized combination of OPW's. For comparison, curve (b) is the true radial wave function of the state.

The radial wave function,[5] $P_{3d}(r)$, corresponding to the $3d$ core state,[2] is plotted in Fig. 1(b); it is shown after multiplication by an orthogonality constant such that it is of just the right amplitude to be subtracted from $rj_2(Kr)$ to orthogonalize the plane waves of this set to the $3d$ core states. The result of the subtraction is shown (after multiplication by a negative constant) in Fig. 2(a), which is then the $l=2$ radial wave function[5] of the lowest symmetrized combination of OPW's.

For comparison, the true radial wave function of the state under consideration is shown in Fig. 2(b). (This is the result of the outward integration of the radial Schrödinger equation for the niobium potential described in Sec. 3A, for the energy of this state as listed in Table VII). It is clear that the lowest symmetrized combination of OPW's is a poor approximation to the

[5] Throughout this paper the term *radial wave function* is used to designate the product of r and the radial component of the wave function. For example, for the wave function $\phi_{nlm}\equiv P_{nl}(r) \times Y_{lm}(\theta,\phi)/r$ the radial wave function is $P_{nl}(r)$.

true wave function. The problem arises because the region of $j_2(Kr)$ for small Kr is involved, where $j_2(Kr)$ has this undersirable shape because of the dominance of the $l(l+1)/(Kr)^2$ term in the defining equation of the spherical Bessel function[6]:

$$\left[\frac{1}{\rho}\frac{d^2}{d\rho^2}\rho+1-\frac{l(l+1)}{\rho^2}\right]j_l(\rho)=0.$$

(Phillips and Kleinman[7] have shown that this term is primarily responsible for the large value of the pseudopotential for $l>0$.) Of course, this problem is also present for $l=1$, resulting in slower convergence of the OPW method for p states than for s states; but the seriousness of the problem obviously increases with increasing l.

Now consider adding to the basis set of OPW's the five functions $P_{4d}^{CO}(r)Y_{2m}(\theta,\phi)/r$ for $m=-2, \cdots, 2$ (where $Y_{lm}(\theta,\phi)$ denotes a spherical harmonic), with $P_{4d}^{CO}(r)$ chosen to have the general form of the atomic $4d$ function except that it is arbitrarily made to vanish at a radius less than half the nearest-neighbor distance; such a function is shown in Fig. 3(a). By taking a linear combination of $P_{4d}^{CO}(r)$ and the radial wave function of the set of OPW's, a function can be produced which is a considerably better approximation to the true wave function; this is shown in Fig. 3.

It is clear for the case considered that the addition of the cutoff (CO) functions to the basis set will improve the convergence considerably. (The CO function is explicitly orthogonalized to the $3d$ core function so that the variational calculation will converge to the conduction-band solutions.) Of course, it is not clear from what has been said that a similar situation would exist for all d-like points throughout the bands, and in particular, that it would be so for a fixed form of P_{4d}^{CO}, independent of energy and wave vector, as is planned here. However, it provides the motivation to try such a procedure, and it turns out that it works quite well (see Sec. 3C).

The trial function is cut off to vanish in the interstitial regions for mathemtical simplicity in computing matrix elements. But the preceding example suggests that such a sharp cutoff is also useful in counteracting the sharp rise of the spherical Bessel function near the zone boundary.

B. Outer Core Functions and OPW's

The plane waves in the OPW method should be orthogonalized to core states which are eigenfunctions of the one-electron conduction-band crystal Hamiltonian. Then, by the variational method, the lowest roots of the secular equation will converge to the conduction-band levels. For simplicity, consider a case in which the crystalline potential V_{cr} is of the muffin-tin form:

$$V_{cr}(\mathbf{r})=\sum_s V(\mathbf{r}-\mathbf{R}_s), \qquad (2.1)$$

where the summation extends over all lattice vectors $\mathbf{R}_s$, and $V(r)$, a spherical potential, vanishes at a value of r less than or equal to r_n, where r_n is half the nearest-neighbor distance. Now consider the bound-state solutions of the Schrödinger equation for the atomiclike potential $V(r)$. If the wave function $\phi_{nlm}(\mathbf{r})$ for such a solution vanishes at a value of $r\leq r_n$, then a tight-binding combination of these orbitals,

$$\sum_s \exp(i\mathbf{k}\cdot\mathbf{R}_s)\phi_{nlm}(\mathbf{r}-\mathbf{R}_s), \qquad (2.2)$$

contains no overlapping functions and is an exact eigenfunction of the crystal Hamiltonian. It is a straightforward procedure to orthogonalize plane waves to these eigenfunctions.[8] However, if the atomiclike solutions extend beyond r_n, then a tight-binding combination contains overlapping functions and is no longer an exact eigenfunction of the crystal Hamiltonian.

For a typical muffin-tin potential for niobium (see Sec. 3A), the $1s$, $2s$, $\cdots$, $3d$ core solutions vanish before r_n (inner-core solutions). However, the $4s$ and $4p$ bound state solutions of $V(r)$ extend out of the cell (outer-core solutions); their radial wave functions are plotted in Figs. 4 and 5, with their tails shown by the dashed lines. The corresponding eigenstates of the crystal Hamiltonian occupy bands of nonzero width, which, in tight-binding language, arise from the overlap of these atomiclike functions. These bands have been calculated for niobium (see Sec. 3D) and are plotted in Figs. 8 and 9. The s and p bandwidths are, respectively, 0.03 and 0.10 Ry. Because it was clear that these bands would be of such an appreciable width, it was decided to proceed in the following way: The plane waves are orthogonalized to the inner-core solutions only. Functions similar to the $4s$ and $4p$ atomiclike states, but modified to vanish

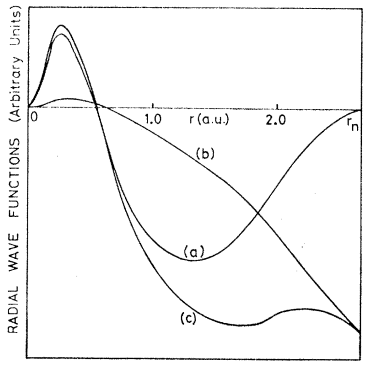

FIG. 3. For the state considered in Figs. 1 and 2: Curve (a) is P_{4d}^{CO}, the CO radial wave function for d conduction states. Curve (b) is the radial wave function of the lowest symmetrized combination of OPW's. A linear combination of (a) and (b) gives (c), an improved approximation to the true state [Fig. 2(b)].

[6] See, e.g., A. Messiah, *Quantum Mechanics* (North-Holland Publishing Company, Amsterdam, 1961), p. 488.
[7] J. C. Phillips and L. Kleinman, Phys. Rev. **116**, 287 (1959).
[8] For presentations of the unmodified OPW method, see T. O. Woodruff, Solid State Phys. **4**, 367 (1957); J. Callaway, *Energy Band Theory* (Academic Press Inc., New York, 1964).

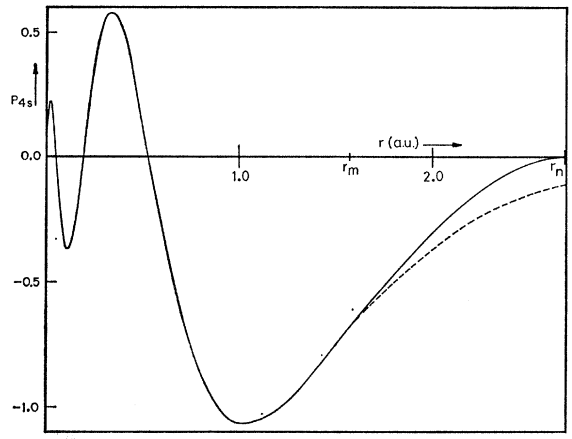

FIG. 4. The 4s atomiclike bound-state solution of the muffin-tin niobium potential has been cut off, as shown by the solid-line tail, to give S_{4s}^{CO} (or P_{4s}^{CO}).

at $r \leq r_n$, are added to the basis set. (As in the case of the 4d CO function, each of these functions is explicitly orthogonalized to the inner-core states.) The solid lines in Figs. 4 and 5 show how these atomiclike solutions have been cut off for niobium. In this way, the core states are calculated explicitly, as the lowest roots of the secular equation in the modified OPW calculation, while higher roots correspond to the conduction-band states. Since the atomiclike 4s and 4p solutions have small amplitudes at the cell boundary, they need be modified only slightly to be converted into CO functions. The calculation then quickly converges to these core band levels by taking optimum linear combinations of the CO functions and the OPW's; when a sufficient number of OPW's have been included to produce convergence to these levels, the conduction-band roots have the same accuracy as if the plane waves had been orthogonalized to the exact wave functions of these core band states.

This procedure for handling the outer-core levels fits simply into an OPW calculation, particularly when CO functions are already being included for d states; it was

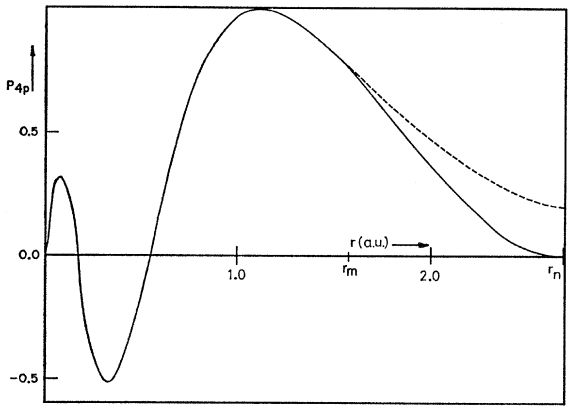

FIG. 5. As in Fig. 4, but for the 4p state.

believed to be better, both for reasons of accuracy and computational simplicity, than the obvious alternative procedure of approximating these outer-core states by tight-binding combinations of overlapping atomiclike orbitals and then either orthogonalizing the plane waves to these tight-binding functions or including these functions in the basis set.

C. The Modified OPW Method

The motivation for the introduction of CO functions has been given above. The basis set for the modified OPW calculation consists of OPW's which have been orthogonalized to the inner-core states only, together with tight-binding combinations of cutoff functions of the form $P_{nl}^{CO}(r)Y_{lm}(\theta,\phi)/r$, corresponding to the outer-core orbitals (4s and 4p for niobium) and the d conduction states (4d for niobium); these CO functions are orthogonalized to the inner-core functions. [Since the $P_{nl}^{CO}(r)$ vanish at a radius less than half the nearest-neighbor distance, tight-binding combinations vanish in the interstitial regions and contain no overlapping of these functions.] The formulation of the CO functions and the derivation of the additional matrix elements required by their addition to the basis set are now given.

The Hamiltonian H is

$$H = T + V_{cr}, \tag{2.3}$$

where T is the kinetic energy operator and V_{cr} is the crystalline potential. Assume that V_{cr} can be expressed in the form

$$V_{cr}(\mathbf{r}) = \sum_s V(\mathbf{r}-\mathbf{R}_s), \tag{2.4}$$

where the atomiclike spherical potentials $V(r)$ centered on different lattice sites may mutually overlap; as in the unmodified OPW method, there is no restriction that the potential be of a muffin-tin form.

For simplicity, in the following derivation it is assumed that the atoms in the solid occupy only the sites of a Bravais lattice. All of the trial functions (OPW's and tight-binding combinations of CO functions) are of the Bloch form; we designate them by $\psi(\mathbf{K})$. It follows that the matrix elements of the Hamiltonian and of unity between any two of these functions contain equal contributions from each cell in the crystal. Hence, in evaluating these matrix elements, only the primitive cell centered at the origin of direct space need be considered, remembering that

$$\langle\psi(\mathbf{K}')|H|\psi(\mathbf{K})\rangle = \langle\psi(\mathbf{K}')|\psi(\mathbf{K})\rangle = 0 \quad \text{for} \quad \mathbf{K}' \neq \mathbf{K}+\mathbf{G},$$

where $\mathbf{G}$ is a reciprocal lattice vector.

Define the OPW's in the cell at the origin by

$$\phi(\mathbf{K}) \equiv (\Omega_0)^{-1/2} e^{i\mathbf{K}\cdot\mathbf{r}} - \sum_{\substack{nlm \\ \text{(core)}}} B_{nl}(K)\psi_{nlm}(\mathbf{r})^{-\frac{1}{2}}, \tag{2.5}$$

where the B_{nl}'s are orthogonality constants given by[8]

$$B_{nl}(K) = F_{nl}(K)Y_{lm}^*(\theta_K,\phi_K), \tag{2.6a}$$

where

$$F_{nl}(K)\equiv 4\pi(\Omega_0)^{-1/2}i^l\int_0^\infty P_{nl}(r)j_l(Kr)rdr. \quad (2.6b)$$

Here Ω_0 is the volume of the primitive cell, $\theta_{\mathbf{K}}$ and $\phi_{\mathbf{K}}$ denote the polar angles of $\mathbf{K}$, $Y_{lm}(\theta,\phi)$ is a spherical harmonic, and $j_l(Kr)$ is the spherical Bessel function. The summation in (2.5) is over the (inner) core states which have wave functions

$$\psi_{nlm}(\mathbf{r})=P_{nl}(r)Y_{lm}(\theta,\phi)/r, \quad (2.7)$$

with normalization

$$\int_0^\infty P_{nl}^2dr=1.$$

Define a CO function in the cell at the origin by

$$\phi_{nlm}^{\mathrm{CO}}(\mathbf{r})\equiv(i)^{-l}P_{nl}^{\mathrm{CO}}(r)\mathcal{Y}_{lm}(\theta,\phi)/r, \quad (2.8)$$

where, for $m>0$,

$$\mathcal{Y}_{lm}(\theta,\phi)=\left[\frac{2l+1}{2\pi}\frac{(l-m)!}{(l+m)!}\right]^{1/2}P_{lm}(\cos\theta)\cos m\phi, \quad (2.9a)$$

$$\mathcal{Y}_{l\bar{m}}(\theta,\phi)=\left[\frac{2l+1}{2\pi}\frac{(l-m)!}{(l+m)!}\right]^{1/2}P_{lm}(\cos\theta)\sin m\phi, \quad (2.9b)$$

and for $m=0$,

$$\mathcal{Y}_{l0}(\theta,\phi)=\left[\frac{2l+1}{4\pi}\right]^{1/2}P_l(\cos\theta). \quad (2.9c)$$

Here $P_{lm}(\cos\theta)$ and $P_l(\cos\theta)$ are, respectively, the associated Legendre function and the Legendre polynomial. [No particular normalization of P_{nl}^{CO} in (2.8) is assumed; normalization is taken care of by the overlap matrix in the variational calculation (see below).] The phase factor $(i)^{-l}$ is included in the definition (2.8) so that matrix elements between OPW's and CO functions are real. In principle, for each radial CO function, P_{nl}^{CO}, it is necessary to include in the basis set the $(2l+1)$ functions $P_{nl}^{\mathrm{CO}}Y_{lm}/r$, thus increasing the order of the secular equation by $(2l+1)$. At symmetry points, however, lattice harmonic combinations of the spherical harmonics can be formed, reducing the dimension of the secular equation. For ease of handling in such cases, the CO functions are defined above in terms of real angular wave functions, $\mathcal{Y}_{lm}$; $\mathcal{Y}_{lm}$ and $\mathcal{Y}_{l\bar{m}}$ are simply independent linear combinations of Y_{lm} and $Y_{l\bar{m}}$.

For mathematical simplicity, the radial functions P_{nl}^{CO} are to be chosen so that they vanish at a radius such that they do not extend into the region of overlap of the spherical potentials [see (2.4)]. For a muffin-tin potential, this radius can be as large as half the nearest-neighbor distance, but it must be smaller in the case of overlapping potentials.

The secular equation to be solved for the energy eigenvalues W is[8]

$$(\mathbf{H}-W\mathbf{S})(\mathbf{A})=0, \quad (2.10)$$

where $\mathbf{H}$ and $\mathbf{S}$ are square matrices with elements

$$H_{ij}=\langle\psi(\mathbf{K}_i)|H|\psi(\mathbf{K}_j)\rangle,$$
$$S_{ij}=\langle\psi(\mathbf{K}_i)|\psi(\mathbf{K}_j)\rangle,$$

and $\mathbf{A}$ is an eigenvector column matrix. W is a solution of (2.10) if the determinant of the coefficients vanishes;

$$\det\|\mathbf{H}-W\mathbf{S}\|=0. \quad (2.11)$$

Schematically, the matrices are of the form

$$\mathbf{H}=\begin{pmatrix}(\mathrm{CO}|H|\mathrm{CO}) & (\mathrm{CO}|H|\mathrm{OPW})\\ (\mathrm{OPW}|H|\mathrm{CO}) & (\mathrm{OPW}|H|\mathrm{OPW})\end{pmatrix}.$$

The OPW-OPW matrix elements are[8]

$$\langle\phi(\mathbf{K}_i)|H|\phi(\mathbf{K}_j)\rangle=K_j^2\delta_{ij}+v(G_{ij})-(4\pi)^{-1}\sum_{nl}(2l+1)\times E_{nl}F_{nl}^*(K_i)F_{nl}(K_j)P_l(\cos\theta_{ij}), \quad (2.12a)$$

$$\langle\phi(\mathbf{K}_i)|\phi(\mathbf{K}_j)\rangle=\delta_{ij}-(4\pi)^{-1}\sum_{nl}(2l+1)F_{nl}^*(K_i)\times F_{nl}(K_j)P_l(\cos\theta_{ij}). \quad (2.12b)$$

Here E_{nl} is the energy of the core state ψ_{nlm}, θ_{ij} is the angle between $\mathbf{K}_i$ and $\mathbf{K}_j$, $\mathbf{G}_{ij}$ is the reciprocal lattice vector joining $\mathbf{K}_i$ to $\mathbf{K}_j$, and $v(G)$ is given by

for $G\neq 0$:

$$v(G)=4\pi(G\Omega_0)^{-1}\int_0^\infty rV(r)\sin(Gr)dr; \quad (2.13a)$$

for $G=0$:

$$v(0)=4\pi(\Omega_0)^{-1}\int_0^\infty r^2V(r)dr. \quad (2.13b)$$

ϕ_{nlm}^{CO} has been chosen so that it is nonzero only in the region where the potential is spherical. The usual separation of variables technique can therefore be used, and the spherical harmonics (and, hence, the real angular wave functions) are eigenfunctions of the angular part of the Hamiltonian. Thus, the effect of the Hamiltonian operating on a CO function can be written as

$$H\phi_{nlm}^{\mathrm{CO}}=H[(i)^{-l}P_{nl}^{\mathrm{CO}}(r)\mathcal{Y}_{lm}(\theta,\phi)/r]=(i)^{-l}E_{nl}^{\mathrm{CO}}G_{nl}^{\mathrm{CO}}(r)\mathcal{Y}_{lm}(\theta,\phi)/r. \quad (2.14)$$

This defines only the product $E_{nl}^{\mathrm{CO}}G_{nl}^{\mathrm{CO}}$; the value of E_{nl}^{CO} can be chosen arbitrarily. [This form is helpful in keeping track of dimensions; the particular values of E_{nl}^{CO} chosen for the niobium calculation have a physical basis (see Appendix C).]

Using the above definitions, the CO-OPW and CO-CO matrix elements are (see Appendix B)

$$\langle\phi_{nlm}{}^{CO}|H|\phi(\mathbf{K})\rangle=(-)^l 4\pi(\Omega_\theta)^{-1/2}E_{nl}{}^{CO}Y_{lm}(\theta_K,\phi_K)\times\int_0^\infty G_{nl}{}^{CO}(r)j_l(Kr)rdr, \quad (2.15a)$$

$$\langle\phi_{nlm}{}^{CO}|\phi(\mathbf{K})\rangle=(-)^l 4\pi(\Omega_0)^{-1/2}Y_{lm}(\theta_K,\phi_K)\times\int_0^\infty P_{nl}{}^{CO}(r)j_l(Kr)rdr, \quad (2.15b)$$

$$\langle\phi_{n'l'm'}{}^{CO}|H|\phi_{nlm}{}^{CO}\rangle=\delta_{ll'}\delta_{mm'}E_{nl}{}^{CO}\times\int_0^\infty P_{n'l'}{}^{CO}(r)G_{nl}{}^{CO}(r)dr, \quad (2.16a)$$

$$\langle\phi_{n'l'm'}{}^{CO}|\phi_{nlm}{}^{CO}\rangle=\delta_{ll'}\delta_{mm'}\times\int_0^\infty P_{n'l'}{}^{CO}(r)P_{nl}{}^{CO}(r)dr. \quad (2.16b)$$

3. APPLICATION TO NIOBIUM

This section describes the application of the above method to calculate the conduction bands along the principal symmetry directions in niobium. The lattice structure is bcc, with lattice constant 3.30A.[9] It is a second-series transition metal, with an atomic configuration, outside closed shells, of $(4d)^4(5s)$.

A. The Potential

As in the unmodified OPW method, a crystalline potential which is expressed as a sum of spherical potentials centered on lattice sites (2.4) can be treated readily by the present method even if the atomiclike potentials mutually overlap. However, in the case of a transition metal there is such uncertainty in the choice of a potential that it is not clear how to construct an overlapping spherical potential that would necessarily be a better approximation to the true crystalline potential than a muffin-tin form. Accordingly, for the purpose of comparison with previous augmented-plane-wave (APW) calculations in other transition metals, a muffin-tin potential has been used for niobium, constructed by a prescription similar to that used by Mattheiss[10] and other authors in APW calculations. In this approximation, free-atom charge densities placed on neighboring lattice sites are considered to overlap. The direct potential contributions are then spherically averaged about a lattice site, and exchange interactions are represented by the Slater free-electron approximation, using a spherical average of the overlapping charge densities. The free-atom charge density was calculated here from the free-atom wave functions computed by Herman and Skillman[11] in the Hartree-Fock-Slater approximation. (The overlap of the first five sets of neighbors was used.) The value of the muffin-tin constant was taken to be the value of the resultant spherical potential at half the nearest-neighbor distance r_n. (This differs from the Mattheiss prescription in which the muffin-tin constant is determined by an averaging procedure, giving a discontinuity in the crystalline potential at r_n; such a discontinuity is easily handled in the APW method, but is unsuitable for OPW calculations.) The muffin-tin constant was then subtracted from this potential, giving finally $V(r)$, which vanishes at r_n. The product $rV(r)$ is listed in Table I.

B. The Core and CO Functions

The bound-state solutions of the atomiclike problem with the potential $V(r)$ have been determined; their energy levels are listed in Table II. The wave functions of the inner-core levels essentially vanish at radii less than r_n; the plane waves are orthogonalized to these levels. The wave functions of the outer core levels, $4s$ and $4p$, are shown in Figs. 4 and 5 for $0\leq r\leq r_n$, with their tails given by the dashed lines. These functions have then been altered to vanish at r_n, as shown by the solid-line tails. (The tails are of a cosine form, as given in Appendix C.) Lastly, these functions have been explicitly orthogonalized to the inner core functions of the same angular momentum to produce the final CO functions, $P_{4s}{}^{CO}$ and $P_{4p}{}^{CO}$. (The orthogonalization does not alter the functions sufficiently to be visible on the scale of these figures.)

For this potential it was found that there is no bound-state solution corresponding to the atomic $4d$ level. Instead, the radial Schrödinger equation was integrated outwards for $l=2$ and $E=1.25$ Ry, giving the function shown in Fig. 6. with the dashed-line tail; this energy was chosen because the resulting wave function is qualitatively of a form that is easily cut off in a smooth, way, but the choice was quite arbitrary. This function was then altered to vanish at r_n, as shown by the solid line in Fig. 6, and then orthogonalized to P_{3d} to yield $P_{4d}{}^{CO}$. (As with the core functions, the orthogonalization does not alter $P_{4d}{}^{CO}$ sufficiently to be visible on the scale of Fig. 6.)

Appendix C gives the analytic form chosen for the CO tails, the method of matching these tails smoothly to the original functions, the procedure for othogonalizing to the inner core states, and the evaluation of the radial function $G_{nl}{}^{CO}(r)$, defined by (2.14).

C. Convergence

The objective has been to obtain convergence of the bands to 0.01 Ry. The maximum possible number of

[9] R. W. G. Wyckoff, *Crystal Structures* (Interscience Publishers, Inc., New York, 1948).
[10] L. F. Mattheiss, Phys. Rev. 133, A1399 (1964).
[11] F. Herman and S. Skillman, *Atomic Structure Calculations* (Prentice-Hall, Inc., Englewood Cliffs, New Jersey, 1963).

TABLE I. Muffin-tin potential for niboium. The value $x=10.46$ corresponds to half the nearest-neighbor distance.

x ($r=0.25675x$, in a.u.)	$rV(x)$ (a.u.$\times Ry$)
0.00	−82.0000
0.01	−81.1273
0.02	−80.2358
0.03	−79.3396
0.04	−78.4481
0.05	−77.5670
0.06	−76.6998
0.07	−75.8485
0.08	−75.0137
0.09	−74.1957
0.10	−73.3943
0.12	−71.8392
0.14	−70.3457
0.16	−68.9114
0.18	−67.5350
0.20	−66.2149
0.22	−64.9487
0.24	−63.7328
0.26	−62.5628
0.28	−61.4342
0.30	−60.3431
0.34	−58.2605
0.38	−56.2955
0.42	−54.4355
0.46	−52.6711
0.50	−50.9944
0.54	−49.3982
0.58	−47.8761
0.62	−46.4229
0.66	−45.0343
0.70	−43.7070
0.78	−41.2258
0.86	−38.9603
0.94	−36.8886
1.02	−34.9857
1.10	−33.2288
1.18	−31.5998
1.26	−30.0856
1.34	−28.6767
1.42	−27.3651
1.50	−26.1435
1.66	−23.2930
1.82	−22.0204
1.98	−20.3254
2.14	−18.8158
2.30	−17.4598
2.46	−16.2355
2.62	−15.1284
2.78	−14.1278
2.94	−13.2236
3.10	−12.4039
3.42	−10.9685
3.74	− 9.7337
4.06	− 8.6434
4.38	− 7.6678
4.70	− 6.7904
5.02	− 6.0001
5.34	− 5.2876
5.66	− 4.6449
5.98	− 4.0643
6.30	− 3.5391
6.94	− 2.6324
7.58	− 1.8875
8.22	− 1.2785
8.86	− 0.7872
9.50	− 0.4009
10.14	− 0.1108
10.46	− 0.0000

TABLE II. The energies of the atomiclike bound-state solutions of the radial Schrödinger equation with the potential given in Table I. The wave functions of the outer-core solutions extend beyond the value of r equal to half the nearest-neighbor distance.

Core	nl	E_{nl} (Ry)
Inner	$1s$	−1358.5
	$2s$	− 187.66
	$2p$	− 173.03
	$3s$	− 30.719
	$3p$	− 25.034
	$3d$	− 14.519
Outer	$4s$	− 3.092
	$4p$	− 1.498

OPW's have been included for each band point, subject to the conditions that the dimension of the unsymmetrized secular matrix not exceed 200 and the dimension of the symmetrized matrix not exceed 50; these

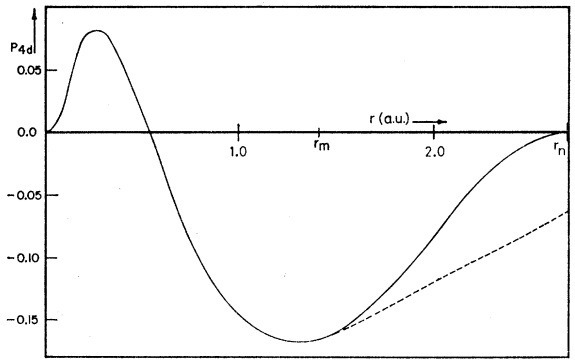

FIG. 6. The function resulting from the integration of the radial Schrödinger equation for $l=2$ and $E=1.25$, for the niobium potential, has been cut off, as shown by the solid-line tail, to give $S_{4d}{}^{CO}$ (or $P_{4d}{}^{CO}$).

conditions simply reflect computer time and storage restrictions. This means that in most cases 150–200 OPW's have been included.

Tables III–V show the degree of convergence at a few representative points. Table III lists the two lowest solu-

TABLE III. The convergence of the energy of Γ_1 (s-like).

No. of OPW's	Dimension of reduced matrix	Lowest eigenvalue (4s core band) (Ry)	Second lowest eigenvalue (conduction band) (Ry)
0	1	−3.018	
1	2	−3.085	0.330
13	3	−3.085	0.328
19	4	−3.089	0.326
43	5	−3.093	0.325
55	6	−3.093	0.325
79	7	−3.100	0.321
87	8	−3.102	0.320
135	9	−3.106	0.318
141	10	−3.106	0.318
153	11	−3.106	0.318
177	12	−3.106	0.318

TABLE IV. The convergence of the energy of H_{15} (p-like).

No. of OPW's	Dimension of reduced matrix	Lowest eigenvalue ($4s$ core band) (Ry)	Second lowest eigenvalue (conduction band) (Ry)
0	1	−1.335	
2	2	−1.468	1.479
10	3	−1.473	1.447
26	5	−1.489	1.429
28	6	−1.490	1.424
52	8	−1.495	1.424
76	10	−1.495	1.421
92	12	−1.503	1.415
108	14	−1.507	1.414
132	16	−1.514	1.409
156	18	−1.517	1.406

tions of the secular equation as more OPW's are added to the basis set for Γ_1, which has s-like symmetry. The lowest root, $E=-3.106$ Ry, belongs to the $4s$ core band which, in tight-binding language, arises from the $4s$ atomiclike state with $E=-3.092$ Ry (see Table II).

TABLE V. The convergence of the energy of $\Gamma_{25'}$ (d-like).

No. of OPW's	Dimension of reduced matrix	Lowest eigenvalue (conduction band) (Ry)
0	1	1.486
4	2	0.786
28	4	0.785
32	5	0.781
40	6	0.775
48	7	0.772
96	10	0.770
100	11	0.769
124	13	0.767
132	14	0.764
156	16	0.760
180	18	0.758

The second lowest solution, $E=0.318$ Ry, is the bottom of the conduction band. Table IV is a similar listing for H_{15} of p-like symmetry. Table V lists the results for the d-like level $\Gamma_{25'}$. The convergence of the s levels appears to be complete to the number of significant

TABLE VI. For some d states, the converged value of the energy is compared with the value resulting when the basis set contains only the CO functions and the lowest symmetrized set of OPW's (2×2 reduced secular equation).

Symmetry of state	k (Units of $2\pi/a$)	E-one set (Ry)	E-converged (Ry)	Deviation (Ry)
H_{12}	(1,0,0)	0.460	0.434	0.026
N_2	$(\frac{1}{2},\frac{1}{2},0)$	0.656	0.612	0.044
Δ_2	$(\frac{1}{2},0,0)$	0.671	0.627	0.044
$\Gamma_{25'}$	(0,0,0)	0.786	0.758	0.028
Γ_{12}	(0,0,0)	1.029	0.932	0.097
N_4	$(\frac{1}{2},\frac{1}{2},0)$	1.120	0.990	0.130
P_3	$(\frac{1}{2},\frac{1}{2},\frac{1}{2})$	1.051	0.998	0.053
$H_{25'}$	(1,0,0)	1.186	1.106	0.080
N_3	$(\frac{1}{2},\frac{1}{2},0)$	1.244	1.159	0.085

TABLE VII. Energy bands of niobium (including outer-core bands)

Symmetry of state	k (units of $2\pi/a$)	No. of OPW's	$4s$ band (Ry)	$4p$ band (Ry)	Conduction-band eigenvalues (Ry)		
Γ_1	(0,0,0)	177	−3.106		0.318		
Γ_{12}	(0,0,0)	192			0.932		
$\Gamma_{25'}$	(0,0,0)	180			0.758		
H_{15}	(1,0,0)	156		−1.517	1.406		
H_{12}	(1,0,0)	196			0.434		
$H_{25'}$	(1,0,0)	184			1.106		
P_3	$(\frac{1}{2},\frac{1}{2},\frac{1}{2})$	192			0.998		
P_4	$(\frac{1}{2},\frac{1}{2},\frac{1}{2})$	192		−1.502	0.645	1.563	
N_1	$(\frac{1}{2},\frac{1}{2},0)$	194	−3.087		0.460	0.956	
N_2	$(\frac{1}{2},\frac{1}{2},0)$	192			0.612		
N_3	$(\frac{1}{2},\frac{1}{2},0)$	196			1.159		
N_4	$(\frac{1}{2},\frac{1}{2},0)$	192			0.990		
$N_{1'}$	$(\frac{1}{2},\frac{1}{2},0)$	198		−1.550	0.873		
Δ_1	$(\frac{1}{8},0,0)$	193	−3.105	−1.460	0.340	0.949	
Δ_1	$(\frac{1}{4},0,0)$	193	−3.101	−1.474	0.400	0.982	
Δ_1	$(\frac{3}{8},0,0)$	193	−3.095	−1.491	0.480	1.025	
Δ_1	$(\frac{1}{2},0,0)$	193	−3.088	−1.505	0.543	1.068	
Δ_1	$(\frac{5}{8},0,0)$	193	−3.082	−1.513	0.551	1.131	
Δ_1	$(\frac{3}{4},0,0)$	193	−3.078	−1.515	0.507	1.236	
Δ_1	$(\frac{7}{8},0,0)$	193	−3.075	−1.513	0.458	1.352	
Δ_2	$(\frac{1}{8},0,0)$	196			0.900		
Δ_2	$(\frac{1}{4},0,0)$	196			0.819		
Δ_2	$(\frac{3}{8},0,0)$	196			0.721		
Δ_2	$(\frac{1}{2},0,0)$	196			0.627		
Δ_2	$(\frac{5}{8},0,0)$	196			0.546		
Δ_2	$(\frac{3}{4},0,0)$	196			0.486		
Δ_2	$(\frac{7}{8},0,0)$	196			0.449		
$\Delta_{2'}$	$(\frac{1}{8},0,0)$	196			0.768		
$\Delta_{2'}$	$(\frac{1}{4},0,0)$	196			0.797		
$\Delta_{2'}$	$(\frac{3}{8},0,0)$	196			0.844		
$\Delta_{2'}$	$(\frac{1}{2},0,0)$	196			0.905		
$\Delta_{2'}$	$(\frac{5}{8},0,0)$	196			0.974		
$\Delta_{2'}$	$(\frac{3}{4},0,0)$	196			1.040		
$\Delta_{2'}$	$(\frac{7}{8},0,0)$	196			1.089		
Δ_5	$(\frac{1}{8},0,0)$	162		−1.458	0.762		
Δ_5	$(\frac{1}{4},0,0)$	162		−1.464	0.759		
Δ_5	$(\frac{3}{8},0,0)$	162		−1.474	0.769		
Δ_5	$(\frac{1}{2},0,0)$	162		−1.485	0.800		
Δ_5	$(\frac{5}{8},0,0)$	162		−1.496	0.860		
Δ_5	$(\frac{3}{4},0,0)$	162		−1.506	0.946		
Δ_5	$(\frac{7}{8},0,0)$	162		−1.512	1.050		
Λ_1	$(\frac{1}{8},\frac{1}{8},\frac{1}{8})$	189	−3.102	−1.477	0.381	0.842	
Λ_1	$(\frac{1}{4},\frac{1}{4},\frac{1}{4})$	189	−3.093	−1.515	0.522	1.059	
Λ_1	$(\frac{3}{8},\frac{3}{8},\frac{3}{8})$	189	−3.087	−1.524	0.652	1.332	
Λ_3	$(\frac{1}{8},\frac{1}{8},\frac{1}{8})$	126		−1.447	0.733	0.934	
Λ_3	$(\frac{1}{4},\frac{1}{4},\frac{1}{4})$	126		−1.456	0.654	0.959	
Λ_3	$(\frac{3}{8},\frac{3}{8},\frac{3}{8})$	126		−1.472	0.623	1.000	
Σ_1	$(\frac{1}{8},\frac{1}{8},0)$	139	−3.103	−1.458	0.361	0.758	0.918
Σ_1	$(\frac{1}{4},\frac{1}{4},0)$	139	−3.096	−1.492	0.453	0.722	0.922
Σ_1	$(\frac{3}{8},\frac{3}{8},0)$	139	−3.088	−1.524	0.476	0.792	0.959
Σ_2	$(\frac{1}{8},\frac{1}{8},0)$	172			0.733		
Σ_2	$(\frac{1}{4},\frac{1}{4},0)$	172			0.678		
Σ_2	$(\frac{3}{8},\frac{3}{8},0)$	172			0.632		
Σ_3	$(\frac{1}{8},\frac{1}{8},0)$	174		−1.460	0.804		
Σ_3	$(\frac{1}{4},\frac{1}{4},0)$	174		−1.471	0.922		
Σ_3	$(\frac{3}{8},\frac{3}{8},0)$	174		−1.480	1.078		
Σ_4	$(\frac{1}{8},\frac{1}{8},0)$	166		−1.455	0.940		
Σ_4	$(\frac{1}{4},\frac{1}{4},0)$	166		−1.456	0.953		
Σ_4	$(\frac{3}{8},\frac{3}{8},0)$	166		−1.456	0.981		

figures shown. As expected, the convergence of the p levels is slower than that of the s levels. In general, the s and p states appear to be converging at a rate similar to their counterparts in OPW calculations in semiconductors.[12,13] The convergence of the d levels seems to be at a rate similar to that of the p levels.

It is difficult to estimate how well converged the p and d states are in the present calculation. Perhaps all that can be said is that their energies might decrease by a further 0.02–0.03 Ry if an infinite number of OPW's were included, although it is probable that they are better converged than that. In this worst case, the d-band levels relative to each other would probably be correct to the desired accuracy of 0.01 Ry, but, since the s levels are apparently fully converged, the s-d band gap at Γ, for instance, would be in error by 0.02–0.03 Ry.

The argument which was presented in Sec. 2A to motivate the addition of an $l=2$ CO function to the basis set is that a linear combination of the CO function and the lowest symmetrized set of OPW's can approximate well the form of a d-band wave function. This is indicated for $\Gamma_{25'}$ by the results listed in Table V, in which the CO function, together with one set of OPW's, gives $E=0.786$ Ry, only 0.03 Ry above the converged value. Table VI lists, for several d-band states, the energies for cases in which the basis set contains only the CO functions and the lowest symmetrized set of OPW's (a 2×2 secular equation in each case), and the deviation of these values from the converged results.[14] The deviation varies over a range of about 0.03–0.10 Ry, and is smaller for the lower bands. The Δ_2 value in this table corresponds to the case presented in Appendix A and shown in Fig. 3; this is probably a representative example for the lower d bands, but for the higher bands this approximation would, apparently, give a wave function which differs more noticeably from the true wave function.

The results discussed above suggest several possible ways of further hastening the convergence. The CO functions might be chosen differently to optimize the convergence throughout the bands (the choice of the functions used here was quite arbitrary); the addition of another set of d functions of the same atomic character but with a different shape for the CO tail might be useful; and the addition of a set of CO functions corresponding to the lowest excited atomic p state ($5p$ for niobium) would almost certainly improve the convergence of p-like band states.

D. Band Structure of Niobium

The conduction-band structure has been computed at the symmetry points Γ, H, P, and N and along the symmetry lines Δ, Λ, and Σ. The results are listed in Table VII, including the $4s$ and $4p$ core bands; only those energies which lie below 1.600 Ry, that is, within 1.282 Ry of the bottom of the conduction band, have been tabulated. The conduction bands are plotted in Fig. 7 and the core bands in Figs. 8 and 9.

The $4s$ and $4p$ core bands have total bandwidths of 0.03 and 0.10 Ry, respectively. It should be remembered that these are the corelike solutions of the conduction-band Hamiltonian, and therefore these bands are expected to be wider than the true core bands. This relatively large width supports the case for treating these states as band states in an OPW calculation, rather than as localized core states.

The conduction bands are very similar to those that have been calculated for the bcc transition metals by the APW method.[15–17] The difference $E(H_{25'})-E(H_{12})$ may be taken as a measure of the d bandwidth: this is

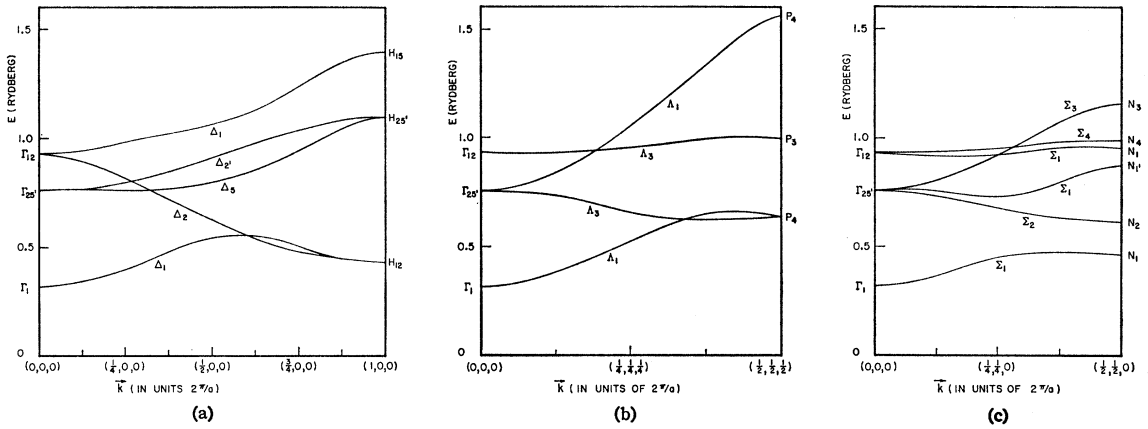

FIG. 7. The niobium conduction bands.

[12] L. Kleinman and J. C. Phillips, Phys. Rev. **116**, 880 (1959).
[13] F. Bassani and M. Yoshimine, Phys. Rev. **130**, 20 (1963).
[14] The term *converged value* is used to designate the energy values listed in Table VII.
[15] J. H. Wood, Phys. Rev. **126**, 517 (1962).
[16] L. F. Mattheiss, Phys. Rev. **134**, A970 (1964).
[17] L. F. Mattheiss, Phys. Rev. **139**, A1893 (1965).

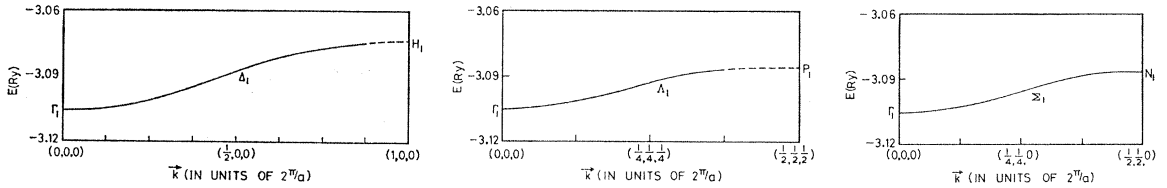

FIG. 8. The 4*s* core bands for niobium. The dashed lines represent interpolation to states for which the core band energies were not calculated.

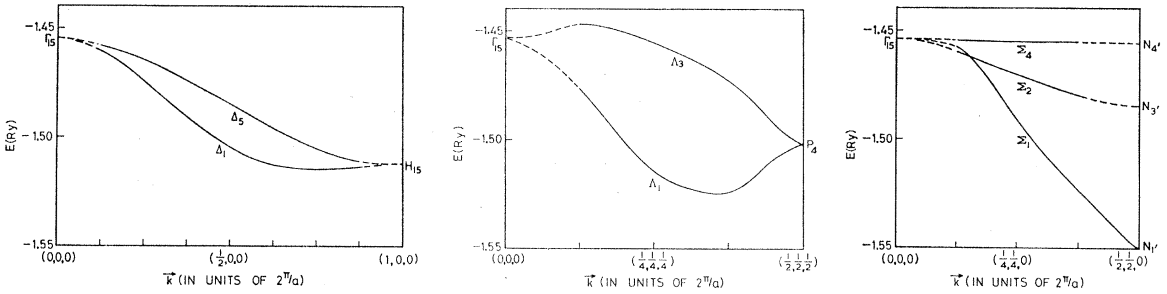

FIG. 9. The 4*p* core bands for niobium. The significance of the dashed lines is given in the caption to Fig. 8.

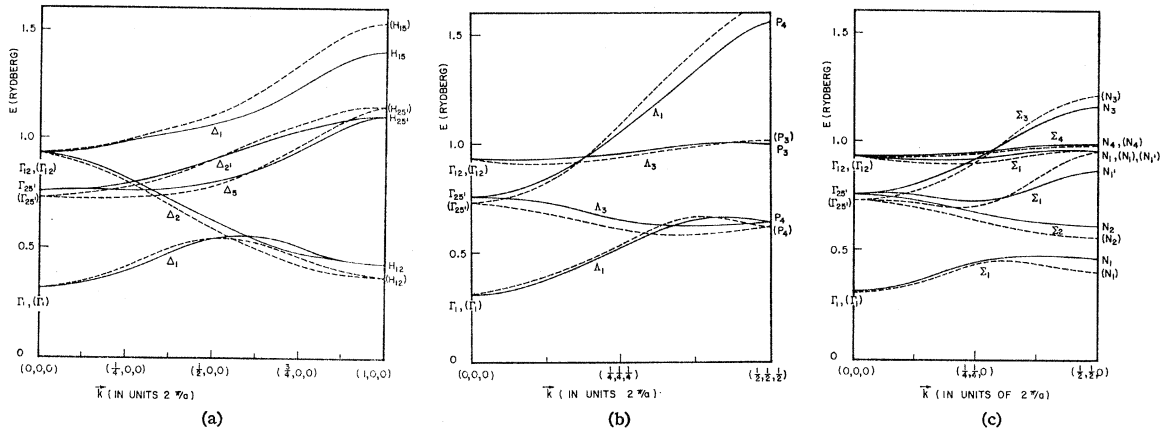

FIG. 10. The conduction bands for niobium (solid lines) are compared with the nonrelativistic conduction bands for tungsten (dashed lines) as computed by Mattheiss, using the APW method(see Ref. 17).

0.67 Ry for the niobium bands, in close agreement with the value 0.68 Ry for molybdenum (a neighbor in the periodic table, also bcc) as determined by Mattheiss[16] by the APW method, using a prescription for the potential similar to that employed here.

The Fermi surface corresponding to these niobium bands was not calculated. However, a Fermi surface for the group-V transition metals (vanadium, niobium, and tantalum) has been calculated by Mattheiss[17] using the nonrelativistic band structure which he obtained for tungsten. The niobium bands are compared with these tungsten bands in Fig. 10. (The main difference is a larger *d* bandwidth for tunsgten, since it is in the third transition series.) Because of the close similarity, the density of states and Fermi surface of niobium that would follow from the bands which are calculated here would probably be qualitatively similar to the group-V calculation based on tungsten. (More to the point, any differences are probably less than the possible error in the Fermi surface due to the uncertainty in the potential.) On this basis the Fermi level is expected to be slightly below $\Gamma_{25'}$.

No relativistic (including spin-orbit) corrections have have been made to the niobium bands. Such corrections would probably be less than 0.01 Ry. (Herman and Skillman[11] calculate the relativistic splitting of the 4*d* level in the niobium free atom to be about 0.015 Ry; for comparison, the Herman and Skillman splitting for the

atomic $5d$ state in tungsten is 0.07 Ry, while the relativistic splitting of the d state $\Gamma_{25'}$ in metallic tungsten has been calculated by the relativistic APW method to be about half this value.)

Because the Fermi level lies near $\Gamma_{25'}$, the shape of the Fermi surface may be sensitive to errors in the band structure due to the uncertainty in the potential; also, as discussed above, $\Gamma_{25'}$ will split relativistically into two levels, Γ_{8^+} and Γ_{7^+}, and this also might lead to deviations from the nonrelativistic predictions.

4. SUMMARY AND DISCUSSION

With the present modifications to the OPW method for transition metal calculations, d states converge at about the same rate as p states; s and p states converge at approximately the same rate as their counterparts in OPW calculations for semiconductors. As in the unmodified method, relatively few OPW's are required to bring the bands to within about 0.05 Ry of convergence, but further convergence proceeds slowly.

The method has been used to calculate the conduction bands in niobium to a convergence of about 0.01 Ry.

The present modifications retain most of the useful characteristics of the OPW method, such as the use of an energy-independent basis set and the ease with which non-muffin-tin potentials can be handled. It may be useful in applications which require explicit use of the wave functions.

ACKNOWLEDGMENTS

This research was proposed by Dr. Twose and was carried out under his supervision. Dr. Twose was actively engaged in the preparation of this manuscript at the time of his sudden death, and the work owes much to his unfailing interest and untiring effort. Helpful discussions, at various states of this work, with Dr. J. P. Carbotte, Dr. L. M. Falicov, Dr. V. Heine, Dr. R. A. Moore, Dr. S. H. Vosko, and Dr. E. J. Woll are gratefully acknowledged.

APPENDIX A. d BANDS AND OPW'S: AN EXAMPLE

This Appendix presents the details of the example which is summarized and discussed in Sec. 2A. For a d-band state in niobium, the lowest symmetrized combination of OPW's is compared with the true wave function of the state; it is shown that the addition of a CO function to the basis set can improve the approximation considerably.

Consider the point $\mathbf{k}=(2\pi/a)(\frac{1}{2},0,0)$ on the Δ_2 band in niobium [see Fig. 7(a)]. For this point, the (unnormalized) symmetrized combination of OPW's which has the wave vector of smallest magnitude is[18]

$$\psi^{\mathrm{OPW}}(\mathbf{r})=\sum_{j=1}^{4} b_j\phi(\mathbf{K}_j),$$

where $\phi(\mathbf{K})$ is an OPW defined by (2.5), $\mathbf{K}_1=(2\pi/a)\times(-\frac{1}{2},-1,0)$, $\mathbf{K}_2=(2\pi/a)(-\frac{1}{2},1,0)$, $\mathbf{K}_3=(2\pi/a)(-\frac{1}{2},0,1)$, $\mathbf{K}_4=(2\pi/a)(-\frac{1}{2},0,-1)$, and $b_1=b_2=1$, $b_3=b_4=-1$. Expanding the plane-wave portion of $\phi(\mathbf{K}_j)$ in spherical harmonics,[19] and using (2.6a) and (2.7):

$$\psi^{\mathrm{OPW}}=\sum_{lm} Y_{lm}(\theta_r,\phi_r)\{4\pi(\Omega_0)^{-1/2}i^l j_l(Kr) - \sum_{n\ (\mathrm{core})} F_{nl}(K)P_{nl}(r)/r\}[\textstyle\sum_j b_j Y_{lm}^*(\theta_j,\phi_j)],$$

where K denotes the magnitude of $\mathbf{K}_j$ (which is the same for all j), (θ_j,ϕ_j) denotes the polar angles of $\mathbf{K}_j$, and (θ_r,ϕ_r) denotes the polar angles of $\mathbf{r}$.

It is readily verified that the quantity in square brackets vanishes for $l=0$ and 1, but is nonvanishing for some m values for $l=2$. These properties simply reflect the fact that the combination has been chosen with the correct symmetry, Δ_2. The $l=2$ component of ψ^{OPW}, denoted by $\psi_d{}^{\mathrm{OPW}}$, is

$$\psi_d{}^{\mathrm{OPW}}=-\{4\pi(\Omega_0)^{-1/2}rj_2(Kr)+F_{3d}(K)P_{3d}(r)\}\times f(\theta_r,\phi_r)/r, \quad \text{(A1)}$$

where the angular function is

$$f(\theta,\phi)\equiv\textstyle\sum_m a_m Y_{2m}(\theta,\phi), \quad \text{(A2)}$$

with

$$a_m\equiv\textstyle\sum_j b_j Y_{2m}^*(\theta_j,\phi_j). \quad \text{(A3)}$$

Equation (A3) simply gives the right coefficients a_m, so that (A2) is the proper $l=2$ lattice harmonic for Δ_2 (although it is unnormalized).

$P_{3d}(r)$ has been determined for the niobium potential (see Sec. 3B) and $F_{3d}(K)$ has been evaluated from (2.6b) by numerical integration. The product $[-F_{3d}(K)P_{3d}(r)]$ is plotted in Fig. 1(b); the quantity $4\pi(\Omega_0)^{-1/2}rj_2(Kr)$ is shown in Fig. 1(a). These have been subtracted to give Fig. 2(a) which, from (A1), is the radial wave function[5] of the $l=2$ component of the lowest symmetrized combination of OPW's. The true $l=2$ radial wave function is shown in Fig. 2(b), obtained by integrating outwards the radial Schrödinger equation with the niobium potential $V(r)$ for $E=0.627$, which is the converged energy value[14] for this state.

Now consider the CO functions defined by (2.8). A linear combination of these functions with the symmetry Δ_2 is

$$\psi_d{}^{\mathrm{CO}}(\mathbf{r})\equiv P_{4d}{}^{\mathrm{CO}}(r)f(\theta_r,\phi_r)/r.$$

The optimum linear combination (unnormalized),

$$\psi_d{}^{\mathrm{CO}}+c\psi_d{}^{\mathrm{OPW}}, \quad \text{(A4)}$$

[18] To obtain the symmetrized combinations of plane waves, see, for example, H. Schlosser, J. Phys. Chem. Solids **23**, 963 (1962).
[19] See, e.g., Ref. 6, p. 497.

for this state is determined by solving the 2×2 secular equation (2.10). The lowest eigenvalue is 0.671 and the corresponding eigenvector gives c in (A4). Fig. 3(a) shows P_{4d}^{CO}; Fig. 3(b) is the product of c and the radial wave function of ψ_d^{OPW} [as shown in Fig. 2(a)]. The addition of these functions gives Fig. 3(c), which is the radial wave function of $(\psi_d^{CO}+c\psi_d^{OPW})$. This is considerably closer to the true result, Fig. 2(b), than is Fig. 2(a).

APPENDIX B. MATRIX ELEMENTS

This Appendix presents the derivation of the matrix elements of the Hamiltonian and of unity between two CO functions and between an OPW and a CO function, resulting in Eqs. (2.15) and (2.16).

The OPW's, $\phi(\mathbf{K})$, are defined by (2.5) and the CO functions $\phi_{nlm}^{CO}(\mathbf{r})$, by (2.8). The Hamiltonian H is given by (2.3) and (2.4). Since the real angular wave function $\mathcal{Y}_{lm}$ can be expressed as a linear combination of spherical harmonics, it is convenient to determine first the matrix elements using the functions ψ_{nlm}^{CO} defined by

$$\psi_{nlm}^{CO}(\mathbf{r})\equiv P_{nl}^{CO}(r)Y_{lm}(\theta,\phi)/r. \tag{B1}$$

From (2.14) it follows that

$$H\psi_{nlm}^{CO}(\mathbf{r})=E_{nl}^{CO}G_{nl}^{CO}(r)Y_{lm}(\theta,\phi)/r. \tag{B2}$$

Therefore,

$$\langle\psi_{n'l'm'}^{CO}|H|\psi_{nlm}^{CO}\rangle$$
$$=\int drd\alpha P_{n'l'}^{CO}Y_{l'm'}^{*}(\theta,\phi)E_{nl}^{CO}G_{nl}^{CO}(r)Y_{lm}(\theta,\phi)$$
$$=E_{nl}^{CO}\delta_{ll'}\delta_{mm'}\int_0^\infty drP_{n'l'}^{CO}(r)G_{nl}^{CO}(r),$$

where $d\alpha\equiv\sin(\theta)d\theta d\phi$. Similarly,

$$\langle\psi_{n'l'm'}^{CO}|\psi_{nlm}^{CO}\rangle=\delta_{ll'}\delta_{mm'}\int_0^\infty drP_{n'l'}^{CO}(r)P_{nl}^{CO}(r).$$

The real angular wave functions can be written

$$\mathcal{Y}_{lm}(\theta,\phi)=a_{lm}Y_{lm}(\theta,\phi)+b_{lm}Y_{l\bar{m}}(\theta,\phi), \tag{B3}$$

where a_{lm} and b_{lm} are chosen to satisfy (2.9). Equations (2.16) immediately follow from (2.8), (B1), and (B3).

Using (2.5),

$$\langle\psi_{nlm}^{CO}|H|\phi(\mathbf{K})\rangle=\langle\psi_{nlm}^{CO}|H|\mathbf{K}\rangle-\sum_{n'l'm'}B_{n'l'}(K)\times\langle\psi_{nlm}^{CO}|H|\psi_{n'l'm'}\rangle,$$

where $|\mathbf{K}\rangle$ is defined by

$$\langle\mathbf{r}|\mathbf{K}\rangle=(\Omega_0)^{-1/2}e^{i\mathbf{K}\cdot\mathbf{r}}.$$

But

$$\langle\psi_{nlm}^{CO}|H|\psi_{n'l'm'}\rangle=E_{n'l'}\langle\psi_{nlm}^{CO}|\psi_{n'l'm'}\rangle=0$$

because the CO functions have been explicitly orthogonalized to the core functions. Hence,

$$\langle\psi_{nlm}^{CO}|H|\phi(\mathbf{K})\rangle=\langle\psi_{nlm}^{CO}|H|\mathbf{K}\rangle$$
$$=E_{nl}^{CO}\int rdrd\alpha\, G_{nl}^{CO}(r)Y_{lm}^{*}(\theta,\phi)\times(\Omega_0)^{-1/2}e^{i\mathbf{K}\cdot\mathbf{r}}.$$

Expanding the plane wave in spherical harmonics,[19] this reduces to

$$4\pi E_{nl}^{CO}(\Omega_0)^{-1/2}i^lY_{lm}^{*}(\theta_K,\phi_K)\int_0^\infty drG_{nl}^{CO}(r)rj_l(Kr).$$

Similarly,

$$\langle\psi_{nlm}^{CO}|\phi(\mathbf{K})\rangle=4\pi(\Omega_0)^{-1/2}i^lY_{lm}^{*}(\theta_K,\phi_K)\times\int_0^\infty drP_{nl}^{CO}(r)rj_l(Kr).$$

Using (2.8), (B1), and (B3), Eqs. (2.15) immediately follow.

APPENDIX C. THE CO FUNCTIONS FOR NIOBIUM

This Appendix presents the form chosen for the CO functions, P_{nl}^{CO}, in the niobium calculation, and the evaluation of $G_{nl}^{CO}(r)$, Eq. (2.14), for this choice. (See also Sec. 3B.)

To determine P_{nl}^{CO}, first integrate the radial Schrödinger equation outwards from $r=0$ for the correct l value for some appropriate energy E_{nl}^{CO}, using the niobium potential. (This defines E_{nl}^{CO} of Eq. (2.14). As discussed in Sec. 3B, the outer core bound-state solutions were used for the $4s$ and $4p$ CO functions, while $E_{nl}^{CO}=1.25$ Ry was chosen for the $4d$.) This function is then cut off at some $r=r_m$ and a tail is joined smoothly to it; the tail is chosen to vanish at $r=r_n$, half the nearest-neighbor distance. Denote by $Q_{nl}^{CO}(r)$ the radial wave function[5] resulting from this integration for the energy E_{nl}^{CO}. The unorthogonalized CO radial wave function, denoted by $S_{nl}^{CO}(r)$, is defined by

$$S_{nl}^{CO}(r)\equiv Q_{nl}^{CO}(r) \quad \text{for} \quad 0\leq r\leq r_m, \tag{C1}$$

and

$$S_{nl}^{CO}(r)\equiv b\{1+\cos[q(r-r_0)]\} \quad \text{for} \quad r_m\leq r\leq r_n. \tag{C2}$$

The three parameters b, q, and r_0 are chosen to satisfy the three conditions that the tail match Q_{nl}^{CO} continuously with continuous first derivative at r_m and vanish identically at r_n. Specifically,

$$b=Q_{nl}^{CO}(r_m)/[1+\cos q(r_m-r_0)], \tag{C3}$$

$$q=\pi/(r_n-r_0), \tag{C4}$$

and r_0 is determined by a trial-and-error procedure; for each trial value of r_0, q is determined by (C4) and then b

TABLE VIII. Parameters for the CO tails.

nl	E_{nl}^{CO} (Ry)	r_n (a.u.)	r_m (a.u.)	r_0 (a.u.)
$4s$	−3.092	2.6856	1.5765	0.6571
$4p$	−1.498	2.6856	1.5765	1.1440
$4d$	+1.250	2.6856	1.4121	1.3350

is then found by (C3). The slopes of (C1) and (C2) are compared at $r=r_m$ and the trial-and-error procedure continues until the slope of (C2) equals that of (C1).

The values of r_m chosen for the niobium cutoff functions are listed in Table VIII, together with the corresponding values of r_0; the resulting functions $S_{nl}^{CO}(r)$ are indicated by the solid lines in Figs. 4, 5, and 6.

There was a great deal of arbitrariness in the choice of the matching points r_m. For the $4s$ (or $4p$) function, r_m corresponds roughly to the beginning of the region where there would be appreciable overlap if the $4s$ (or $4p$) bound-state wave functions were placed on nearest-neighbor lattice sites. For the $4d$ function, r_m was chosen to be slightly greater than the value of r corresponding to the peak of Q_{4d}^{CO}.

Each CO function must now be orthogonalized to the inner-core functions, so the final (orthogonalized) CO function is

$$P_{nl}^{CO}(r)=S_{nl}^{CO}(r)-\sum_{n'} a_{n'l}^{CO}P_{n'l}(r), \qquad \text{(C5)}$$

where

$$a_{n'l}^{CO}=\int_0^\infty P_{n'l}(r)S_{nl}^{CO}(r)dr,$$

and the summation is over inner-core states of angular momentum l.

The effect of operating on a CO function with the Hamiltonian is now shown. Define ψ_{nlm}^{CO} by Eq. (B1). Then, for $0\leq r\leq r_m$: From (C5) and (C1),

$$H\psi_{nlm}^{CO}=H(Q_{nl}^{CO}(r)-\sum_{n'} a_{n'l}^{CO}P_{n'l}(r))Y_{lm}(\theta,\phi)/r$$
$$=(E_{nl}^{CO}(r)Q_{nl}^{CO}(r)-\sum_{n'} E_{n'l}a_{n'l}^{CO}P_{n'l}(r))\times Y_{lm}(\theta,\phi)/r.$$

Then, from (B2)

$$G_{nl}^{CO}(r)=Q_{nl}^{CO}(r)-(E_{nl}^{CO})^{-1}\sum_{n'} E_{n'l}a_{n'l}^{CO}P_{n'l}(r).$$

For $r_m\leq r\leq r_n$: From (C5) and (C2),

$$H\psi_{nlm}^{CO}(r)=\mathrm{I}+\mathrm{II},$$

where

$$\mathrm{I}\equiv H\{b[1+\cos q(r-r_0)]Y_{lm}(\theta,\phi)/r\}$$

and

$$\mathrm{II}=H\{-\textstyle\sum_{n'l}a_{n'l}^{CO}P_{n'l}(r)Y_{lm}(\theta,\phi)/r\}.$$

Immediately,

$$\mathrm{II}=-\textstyle\sum_{n'} E_{n'l}a_{n'l}^{CO}P_{n'l}(r)Y_{lm}(\theta,\phi)/r.$$

Also,

$$\mathrm{I}=\{-\nabla^2+V(r)\}\{b[1+\cos q(r-r_0)]Y_{lm}(\theta,\phi)/r\}$$
$$=\frac{Y_{lm}(\theta,\phi)}{r}\left\{-\frac{d^2}{dr^2}+\frac{l(l+1)}{r^2}+V(r)\right\}\{b[1+\cos q(r-r_0)]\}$$
$$=\frac{Y_{lm}(\theta,\phi)}{r}\left\{bq^2\cos q(r-r_0)+b[1+\cos q(r-r_0)]\times\left[\frac{l(l+1)}{r^2}+V(r)\right]\right\}.$$

Therefore,

$$G_{nl}^{CO}(r)=\frac{1}{E_{nl}^{CO}}\left\{bq^2\cos q(r-r_0)+b[1+\cos q(r-r_0)]\times\left[\frac{l(l+1)}{r^2}+V(r)\right]-\sum_{n'} E_{n'l}a_{n'l}^{CO}P_{n'l}(r)\right\}.$$

Note that only the first derivative of the tail of the CO function has been matched at $r=r_m$. This means that, in general, the second derivative is discontinuous at r_m as well as at r_n. (At the latter point the tail is a cosine function at its extremum and therefore has a nonvanishing second derivative.) These discontinuities must be kept in mind when applying the kinetic-energy operator to the CO function; specifically, G_{nl}^{CO} has finite discontinuities at these points and so the integrals involving G_{nl}^{CO} must be evaluated accordingly.